Environmental Engineering and Management Journal *April 2019, Vol. 18, No. 4, 907-920*
http://www.eemj.icpm.tuiasi.ro/; http://www.eemj.eu

"Gheorghe Asachi" Technical University of Iasi, Romania

MODELLING THE SOURCE TERM FOR POLLUTANTS GENERATED FROM GALVANIC CELLS

Marco Barozzi[1], Marco Ragazzi[2], Sabrina Copelli[1], Vincenzo Torretta[3], Fabio Conti[3], Elena Cristina Rada[2,3,4*], Lucian Ionel Cioca[4,5], Daniele Rizzini[6]

[1]University of Insubria, Department of High Technology Sciences, 46 Via G.B. Vico, 21100 Varese, Italy
[2]University of Trento, Department of Civil, Environmental and Mechanic Engineering, 77 via Mesiano, I-38123 Trento, Italy
[3]University of Insubria, Department of Theoretical and Applied Sciences, 46 Via G.B. Vico, 21100 Varese, Italy
[4]Lucian Blaga University of Sibiu, Department of Industrial Engineering and Management, Faculty of Engineering, 4 Emil Cioran Street, 550025 Sibiu, Romania
[5]Academy of Romanian Scientists, 54 Splaiul Independentei, District 5, 050094 Bucharest, Romania
[6]Politecnico di Milano, Department of Chemistry Materials and Chemical Engineering "G. Natta", 32 Piazza L. da Vinci, 20133 Milano, Italy

Abstract

Being able to estimate the quantity of pollutants that can be spread in the environment is a factor of paramount importance in the industrial panorama. In order to accomplish such aim, a crucial step is the estimation of the so-called source term, that is the rate of generation (or release) of a substance in a generic process. A proper estimation requires to consider both the machinery and the unit operations present into the analysed system. For such reasons, ad hoc considerations and models should be developed for each specific process, in order to represent the reality in the most consistent way. In this paper, a process of the galvanic industry has been taken into account. Specifically, we propose a possible theoretical method for estimating the term of generation from a group of electrolytic deposition tanks. The model is based upon modelling the rupture of bubbles which are formed during the process. The model was applied in order to estimate the pollutants concentration inside the extraction line the and inside the facility. Results have been compared to experimental measurements. Particularly, it has been observed a good agreement between experimental and predicted concentrations for what concerns sulphuric acid and nickel; some deviations can be observed for compounds as nitric acid. This is mainly due to the particular nature of this substance. In fact, nitric acid is subjected to some decomposition reactions which have not be taken into account in the evaporation model. This aspect could be analyzed in future works.

Key words: electrolytic tanks, galvanic industry, generation term, harmful indoor emissions

Received: September, 2018; Revised final: January, 2019; Accepted: April, 2019; Published in final edited form: April, 2019

1. Introduction

During the last years, the interest for environmental pollution and its negative effects on human health has risen remarkably (Cioca et al., 2010; 2015; Călămar et al., 2016; Jang et al., 2017; Matarazzo et al., 2018; Schiavon et al., 2018; Stefan et al., 2015; Shareefdeen and Singh, 2004; Schiavon et al., 2016; Torretta et al., 2015). Intensive studies have been carried out, with the aim to protecting the life of both the industrial workers and the people involved, either directly or indirectly in both acute and chronical intoxications (Cioca and Ivascu 2016; Călămar et al., 2018; Fontcha et al., 2015; Junaid et al., 2016; Oprea et al., 2017; Rada et al., 2014; Simion et al., 2017). In industrial environments, the dispersion of polluting substances and accidents are an extremely complex topics to study (Bergstra et al., 2018; Călămar et al., 2017; Cocarta et al., 2009; Moraru et al., 2014; Torretta et al., 2015). In fact, it is highly

* Author to whom all correspondence should be addressed: e-mail: elena.rada@unitn.it; Phone: +390332218782; Fax: +390332218779

influenced by both the nature of the harmful substance and the specific device or instrument that causes the dispersion of the same. For example, the same liquid can be spread into the environment as a fine spray or in form of bigger drops, because of the different operations carried out on the liquid to be processed. This feature is what makes the modeling of air-pollutants dispersion in industrial environments a complex and challenging argument. In general, most of the mathematical models used to predict the dispersion of a substance, highly rely on the determination of the so-called *source ter*m (or term of generation). This is, namely, a quantity that describes the mass flow of the analyzed pollutant into the environment. A proper definition of the term of generation requires the modeling of all the physical phenomena related to the process.

In this work, the focus is on a specific galvanic process. In the current literature, many works involved in the estimation of the source term in galvanic industries are found (DSEWPC, 2012; TCEQ, 2018; USEPA, 1995). Fig. 1 offers a list of all the possible substances participating in the definition of the source term in a galvanic process. A correct definition of the term of generation should take into account all of these listed pollutants. This is the reason which explains why, actually, there is not a single general model applied to evaluate the dispersion of a harmful agent, but a pattern of more particular, specific techniques is proposed instead. The *Emission Estimation Technique Manual for Galvanizing*, lists four main categories of methods used to estimate the source term:

1. Sampling data or direct measurement
2. Mass balance
3. Fuel analysis or engineering calculations
4. Emission factor

As already stated, no general criteria are given for a priori choice of the best technique. In general, a mix of the proposed models can be the right answer, but, more often, the correct selection is driven by the amount of data available and collectable, as by the degree of precision required for the analysis.

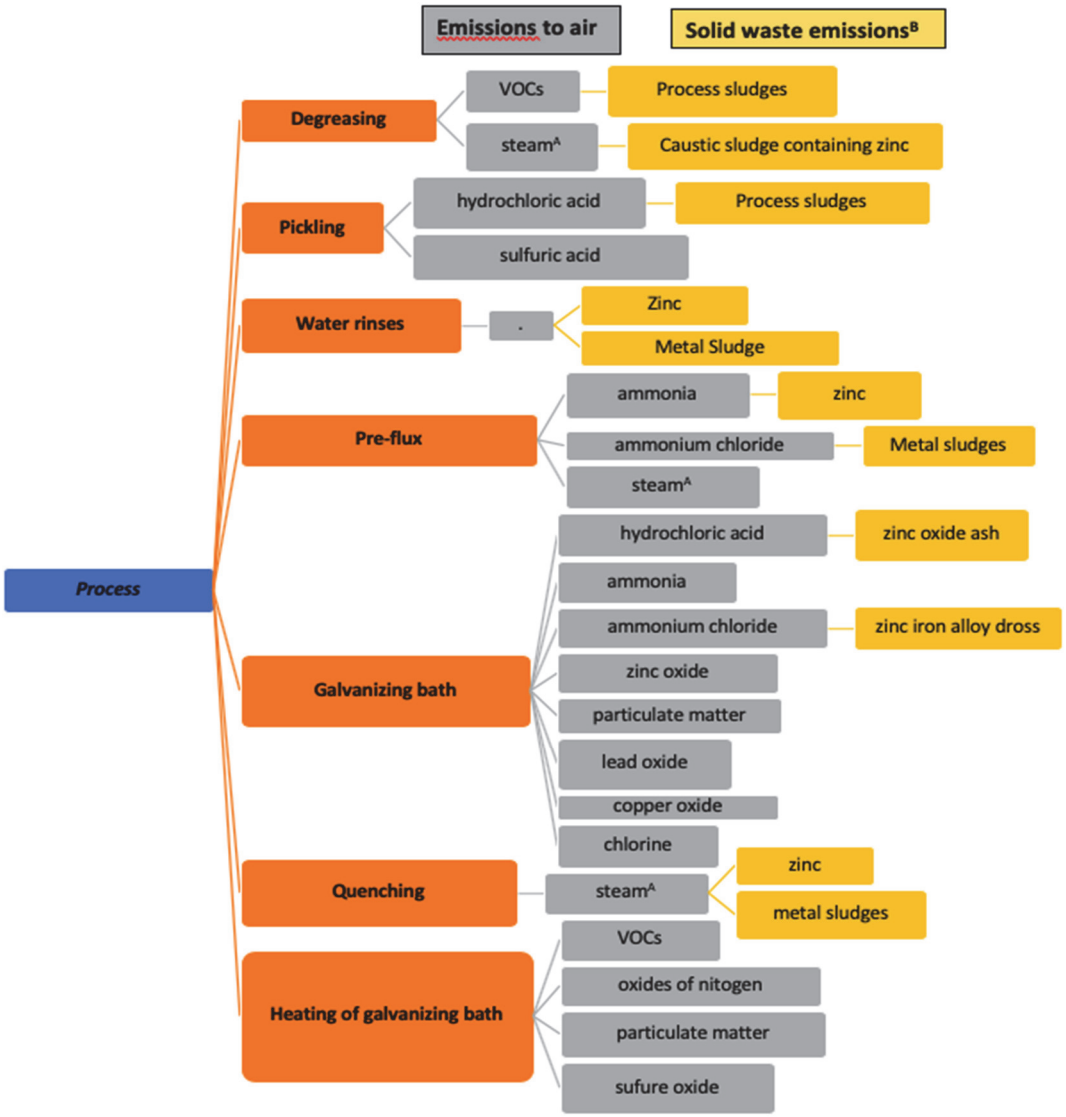

A. Non NPI (National Pollutant Inventory) substance
B. May result in the transfer of NPI substances

Fig. 1. Material input and emissions from galvanizing processes (updated upon DEHP, 1998)

The purpose of this work is to propose a model for estimating the term of generation in a process of the galvanic industry. The results of the model have been then compared with experimental data, collected by direct sampling in the indoor environment of the analyzed facility, showing interesting outputs.

2. Material and methods

The case study focuses on the determination of the source term in a galvanization process, specifically two aluminium passivation methods: anodizing and chromate conversion. Anodizing is among the most efficient protection techniques for light metals and it has found several applications in a lot of commercial products. The main target of this treatment is to increase the resistance to corrosion and wear, providing better adhesion for paint primers and glues than the starting metal. Anodizing is an electrolytic passivation of a metal, which is increasing the thickness of the natural oxide layer on the surface of the same. The most common application is on aluminium, the context of this work. By the other side, chromate conversion coating covers the surface of the aluminium substrate with a trivalent chromium layer. The thickness of the chromium coating is around 0.5 microns. Chromate conversion grants high corrosion resistance and maintains the electrical conductivity of aluminium. The facility object of this study operates with both processes.

The anodizing process is made of the following steps (Diggle et al., 1969):

- Sulfuric acid concentration
- Bath temperature
- Residence time
- Cathode position
- Stirring in the bath
- The industrial process is usually organized in the following phases:
  - *Disposition of the material in the bath:* the aluminum components which will be anodized are set in place;
  - *Degreasing*: alcohols and acids solutions are used to clean the aluminium surface from residuals coming from previous treatments;
  - *Chemical etching*: with the addition of a caustic soda solution, the surface of the metal is smoothed;
  - *Acid neutralization*: before starting the oxidation process, the pH of the bath must be neutralized;
  - *Sulfuric acid oxidation*: the treated component is put into the sulfuric acid bath, where the anodizing takes place;
  - *Coloring*: this part is optional, through the application of metal salts, the surface of the anodized aluminium gets colored;
  - *Sealing*: the final phase, the pores generated by the oxidation process are sealed with precipitation of nichel salts;
  - *Drying*.

In the case of chromate conversion, the industrial iter is almost the same, expection made for the oxidation in sulfuric acid, which here it is substituted by incolor or yellow chromium conversion coating (Volk, 2013).

The aforementioned processes are performed inside the facility considered in this work, represented in Fig. 2. Looking at Fig. 2, it is possible to notice the two lines (blue) where the passivation treatments are operated. Particularly, they are arranged in parallel rows, separated by a catwalk (green). The structure is 7 meters high, while the dimensions of the trapezium (form of the indoor environment) are 36.53 m and 29.61 m for the basis, and 24.68 m as height. All the 39 installed tanks (blue) have similar dimensions: they are 1.4 m high, 3.3 m long and between 0.85 m and 0.75 m thick. Fig. 3 shows the structure of one of the anodizing tanks.

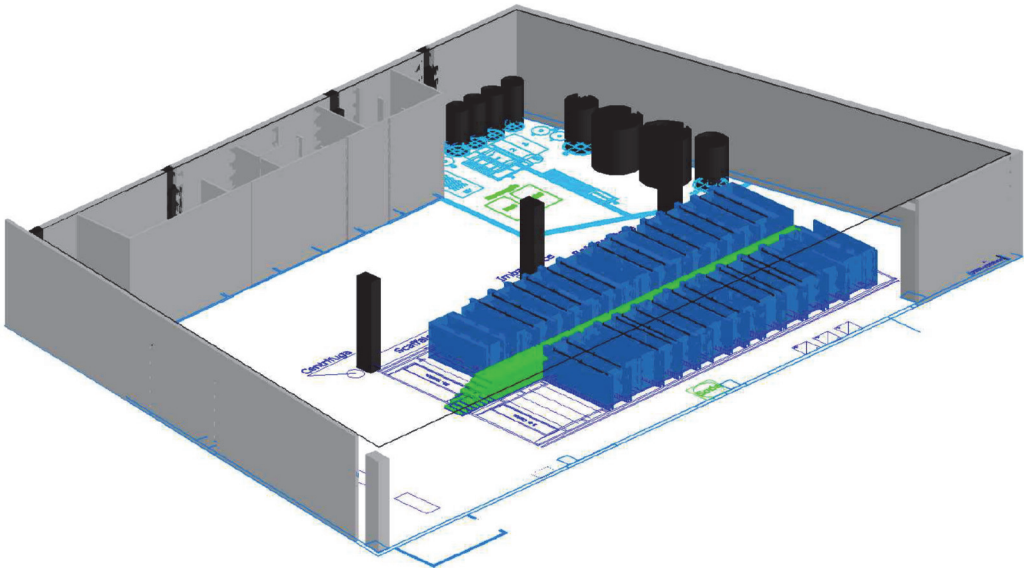

Fig. 2. Tridimensional view of the facility studied

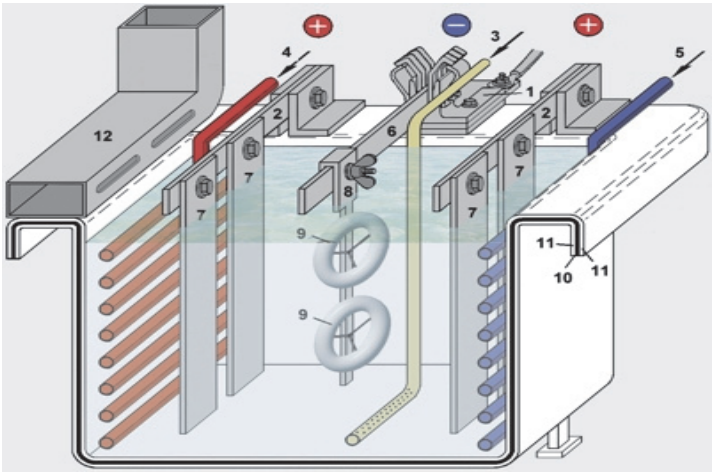

Fig. 3. Anodizing bath
(1 - Cathode connection; 2 - Anodic bar with connections; 3 - Air inlet for stirring; 4-5 - Temperature adjustment; 6 - Bar for works hanging; 7 – Cathode; 8 - Rack; 9 – Works; 10 - Steel container; 11 - Corrosion resistant coating; 12 - Extraction system)

The tank contains the electrolytic cell where the elecrolytic reaction takes place. It is possible to see that the cathode and the anode are fixed on lateral places, and the sparger for the mixing air is located on the bottom of the tank. Both personal and environmental samplers have been used in order to estimate pollutants dispersion inside the facility.

2.1. Sampling

In order to compare the results of the proposed model with real data, a sampling procedure was applied for: inorganic acids, nickel and chromium ions. Both environmental and personal air samplers have been used to evaluate pollutants concentrations. Samples have been collected and analyzed with ionic exchange HPLC. All the procedures have been performed in accordance with the UNI EN 689:1997 standard.

2.2. Model description

Two models developed to describe the source term are presented. As it emerges from the operations description, the pollutants involved in the industrial process are inorganic acids and metal ions. Thus, the source term comes from the release of vapors from the baths. The first model proposed is intended as a simplified one, since it takes in account only the evaporation as the cause of the release of agents in the surrounding indoor environment. The second model is more accurate, describing the physics of the bubbles that break upon reaching the liquid surface, and it should be the correct estimator of the generation term.

2.2.1. Pure evaporation model

At first, a relatively simple model can be developed by considering the generation of vapors by evaporation from the anodizing bath only. Thus, a standard vapor-liquid equilibrium state is evaluated. The gaseous phase will be treated as an ideal gas. For this purpose, a generic tank will be considered, where spargers are located on the bottom of the tank and they spread bubbles directly inside the solution. The air extraction is situated on the top-side parts of the bath.

According to this scheme, it is possible to write a material balance equation (Eq. 1) on a generic pollutant, named α, considering as control volume the portion of the space among the liquid and the walls of the tank (Goodfellow and Tähti, 2001).

$$acc = in - out + prod \tag{1}$$

where:

- *acc* is the accumulation term (Eq. 2), that is the variation of the mass of the element α in the control volume (which is considered constant), in time.

$$acc = \frac{d(m_\alpha)}{dt} = \frac{d(C_\alpha \cdot PM_\alpha \cdot V)}{dt} = V \cdot PM_\alpha \cdot \frac{d(C_\alpha)}{dt} \tag{2}$$

- *in* is the inlet material flow rate of component α inside the control volume (Eq. 3). Here two contributions must be treated: the flow rate of α coming from the outside air, and the flow rate coming from the recirculation air of the ventilation system. The first amount can be considered negligible, the second one can be evaluated considering the air saturated with α vapors, that is in a liquid-gas equilibrium

$$in = Q_{air_{mix}} \cdot \frac{\overline{RT}}{P} \cdot \frac{P_\alpha^0}{P} \cdot PM_\alpha \tag{3}$$

- *out* is the outside mass flow rate of α, represented by the ventilation system that drags it away (Eq. 4).

$$out = Q_{extr} \cdot C_\alpha \cdot PM_\alpha \tag{4}$$

- *prod* is, at last, a production term (Eqs. 5-6); in our case it can be acknowledged as it is an evaporating pool (Perry and Green, 2007):

$$prod = k_p \cdot PM_\alpha \cdot (P_\alpha^0 - P \cdot y_\alpha) \cdot S_{evap} \quad (5)$$

$$y_\alpha = \frac{\overline{RT}}{P} \cdot C_\alpha \quad (6)$$

The material balance equation (Eq. 7) can be then rewritten as:

$$V \cdot PM_\alpha \cdot \frac{d(C_\alpha)}{dt} = Q_{air_{mix}} \cdot \frac{\overline{RT}}{P} \cdot \frac{P_\alpha^0}{P} \cdot PM_\alpha - Q_{extr} \cdot C_\alpha \cdot PM_\alpha + k_p \cdot PM_\alpha \cdot (P_\alpha^0 - P \cdot \frac{\overline{RT}}{P} \cdot C_\alpha) \cdot S_{evap} \quad (7)$$

Since all the terms outside C_α, can be reasonably assumed as constants, Eq. (7) is a linear, first order differential equation, with the following initial condition (Eq. 8):

$$C_\alpha(t=0) = C_\alpha^0 = 0 \quad (8)$$

The analytical solution of the equation is given by Eq. (9):

$$C_\alpha(t) = \frac{A}{B} \cdot (1 - \exp(-B \cdot t)) \quad (9)$$

where (Eqs. 10-11):

$$A = \frac{k_p \cdot S_{evap}}{V} \cdot P_\alpha^0 + \frac{Q_{air_{mix}}}{V} \cdot \frac{\overline{RT}}{P} \cdot \frac{P_\alpha^0}{P} \quad (10)$$

$$B = \frac{k_p \cdot \overline{RT} \cdot S_{evap}}{V} \cdot P_\alpha^0 + \frac{Q_{extr}}{V} \quad (11)$$

It is possible to notice that, in this model, the source term depends on both the extraction of air by the ventilation system and the mixing inside the volume of liquid. Thus, for such reasons, the concentration of the pollutant α results always diluted, and it never reaches the saturation concentration $P_\alpha^0/\overline{R}\,T$, but the ratio A/B. The results of this model, indeed, do not give good matches with the experimental data. Therefore, it is necessary to take into account other physical effects in order to estimate correctly the source term.

2.2.2. Bubble rupture model

In order to obtain a more realistic model, is it necessary to model the physics of the bubbles involved in the release of pollutants in the galvanizing bath. We assume the following mechanism for the aersol formation: once spread from the sparger, bubbles rise through the liquid, generating turbulence, and they allow the stirring required for the process. On the top of the liquid, bubbles will break. The correct evaluation of the aerosol composition requires the characterization of the fluid dynamics of the system involved. The first step is the estimate of size of the bubbles generated by the sparger. This is done by an empiric correlation (Kumar and Kuloor, 1970), based on the properties of the liquid and the geometry of the sparger (Eq. 12):

$$\frac{d_b}{d_0} = 3.23 \left(\frac{4\mu_l Q_{air_{mix}}}{\pi \rho_l d_0} \right)^{-0.1} \left(\frac{Q_{air_{mix}}^{\ 2}}{g \cdot d_0^5} \right)^{-0.1} \quad (12)$$

While rising through the liquid, it is possible to assume that their size is rearranged, according to a Poisson distribution (Eq. 13):

$$P(y) = \frac{d_b^{\ y}}{y!} \exp(-d_b) \quad (13)$$

While emerging through the solution, bubbles will be affected by the presence of the liquid which surrounds them. This brings to a modification of their shape. Thus, all properties and physical quantities related to bubbles, will be evaluated based that on their radius of curvature R (Lhuissier and Villermaux, 2012).

A bubble breaks upon the nucleation of a hole on its cup. The dynamic of this rupture highly depends on the limit thickness (h_b) of the cup itself at the moment of the rupture: in an initial phase the drainage of the liquid film at the base of the bubble occurs, followed by the hole nucleation on the surface, which then starts to propagate, leading to the rupture of the cup, that causes the scattering of drops that constitutes the aerosol. In the following, all phases involved with the bubbles rupture will be analyzed.

Drainage

A gas bubble can be considered as a curve, thin liquid film, with some gas inside of it, bounded by the liquid surface thanks to a convex meniscus, as shown in Fig. 4. The drainage phase takes a relative long time in the whole rupture process. The main influencing factor here is the shape of the bubble, which affects how the gravity force insists on the liquid film, and the capillary pressure on the curvature of the cup. We can assume, for simplicity sake, that the shape of the cup, due to the hydrostatic balance, is a half sphere (Lhuissier and Villermaux, 2012). The buoyancy force is then (Eq. 14) (Lhuissier and Villermaux, 2012):

$$F_b = \rho \cdot g \cdot \frac{4\pi}{3} \left(\frac{R}{2} \right)^3 \quad (14)$$

Which is equaled by the vertical component of the surface tension insisting on the base of the bubble (Eqs. 15-16) (Lhuissier and Villermaux, 2012).

$$F_{sur} = \sigma \cdot \sin(\theta_c) \cdot 2\pi \cdot R \cdot \sin(\theta_c) \quad (15)$$

where:

$$\lim_{\frac{R}{a} \to 0} (\theta_c) = \frac{R}{2\sqrt{3}a} \quad (16)$$

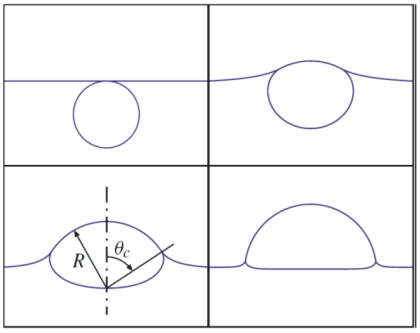

Fig. 4. Bubble shapes with different radius R and characteristic angles θ_C (Lhuissier and Villermaux, 2012)

After reaching the liquid surface, the film with be at a higher level than the surface, here then starts he drainage of liquid from the top of the couple to its base, bringing to a gradual reduction of the film thickness. This effect is driven by gradient between the capillar pressure and the hydrostatic one. They highly depend on the ratio R over a, from that we can deduce that for bubbles with radius $R<5a$, the capillary pressure is dominant. The drainage can be then divided in two steps: inertial and viscous. At first, we have a flow of liquid dropping on the bubble surface, followed by the viscous phase. Here we have convenctive motions over the film, with the formation of convective cells, which makes the film uniform, with an homogeneus film thickness on almost the whole bubble. At last, the average film thickness h can be expressed by the following (Eq. 17):

$$h = F(\theta)\sqrt{\frac{4\eta}{\rho \cdot g \cdot R \cdot t}} \tag{17}$$

$F(\theta)$ does not depend on the cap extension θc (Lhuissier and Villermaux, 2012), and its value is assumed 1 for θ=0 and 0.76 for θ=π/2.

Pinching

During the drainage phase, it is possible that the liquid flows on the bubble surface producing a local thinning of the film, weakening its resistance. As it is possible see in Fig. 5, a pinching occurs over an arc length l, with a local minimum thickness δ.

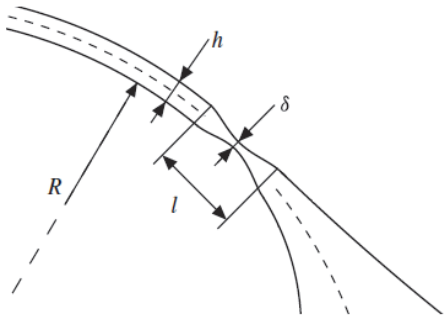

Fig. 5. Schematization of a pinching on the liquid film of a baubble (Lhuissier and Villermaux, 2012)

Experimental evidences (Lhuissier and Villermaux, 2012; Nierstrasz et al., 1998) confirm the following assumptions:

- The pinching phenomenon occurs about 10^{-2} seconds after the emerging of the bubble;
- It lasts for the whole bubble lifetime;
- The pinching neck thickness δ is never below half the width of the film.

Puncturing

Due to the continue thinning of the bubble film, a hole will form, leading to a subsequent rupture of the bubble itself. This hole nucleation often appears to occur near the base of the bubble. The limit film thickness h_b, under similar conditions to those of the process studied, according to empirical data, follows this law (Eq. 18) (Lhuissier and Villermaux, 2012; Spiel, 1998):

$$h_b = \frac{R^2}{\ell} \tag{18}$$

where ℓ is a characteristic length, which will be discussed later.

From experimental data (Lhuissier and Villermaux, 2012; Spiel, 1998), the following informations are well known:

- The limit thickness highly depends on the bubble radius R;
- h_b is independent from the contents of the bubble, exception made for a high emulsifier concentration;
- the hole nucleation starts almost always at the bottom of the bubble.

Another important parameter is the puncture efficiency ε. The holes nucleate in an unstable convection cell, but it seems that rarely this hole instantly causes the rupture of the bubble. From experimental evidence (Lhuissier and Villermaux, 2012) only 1 puncture over thousand/ten thousand brings the bubble to break up. Thus (Eq. 19):

$$\varepsilon = 10^{-3} - 10^{-4} \tag{19}$$

For what concerns the characteristic length ℓ, it has found to be solely function of the capillary length scale, and differing from it by a very large amount depending on the puncture efficiency factor (Eq. 20) (Lhuissier and Villermaux, 2012).

$$\ell \approx \frac{a}{\varepsilon^{\frac{1}{2}}} \tag{20}$$

Fragmentation

Fig. 6 shows some steps of the fragmentation of a bubble. In this phase the hole generated during the puncturing propagates and leads to the complete bubble breakage. This phase is crucial to the following formation of an aerosol. Thus, it is important to model

this correctly, in order to achieve a reliable model for the source term.

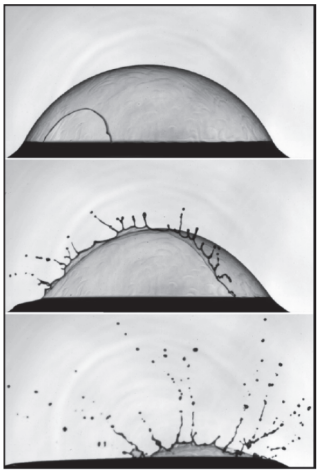

Fig. 6. Fragmentation of a bubble (1 mm radius and 3.1 μm thickness) (Lhuissier and Villermaux, 2012)

The expansion of the hole to the entire bubble surface is a very fast phenomenon. The expansion velocity v and the centripetal acceleration γ, can be estimated by the following (Eqs. 21-22):

$$v = \left(\frac{2\sigma}{\rho \cdot h} \right)^{\frac{1}{2}} \tag{21}$$

$$\gamma = \frac{v^2}{R} \tag{22}$$

where: v is the well-known Taylor-Culick velocity (Culick, 1960), and it is constant. Two additional terms are defined: the instability wavelength λ (Lhuissier and Villermaux, 2012) and the characteristic capillary time based on the instability wavelength τ. The meaning of λ (Eq. 23) is the distance between two nearby waves that generate during the bubble rupture, and it is the geometrical mean of R and h.

$$\lambda \approx \sqrt{\frac{\sigma}{\rho \cdot \gamma}} \approx \sqrt{R \cdot h} \tag{23}$$

For water (Eqs. 24-26):

$$\lambda = 4\sqrt{R \cdot h} \tag{24}$$

and

$$\tau \approx \sqrt[4]{\frac{\sigma}{\rho \cdot \gamma^2}} \approx \sqrt{\frac{\rho \cdot (R \cdot h)^{\frac{3}{2}}}{\sigma}} \tag{25}$$

$$\tau = 1.8\sqrt{\frac{\rho \cdot (R \cdot h)^{\frac{3}{2}}}{\sigma}} \tag{26}$$

The time at which the first drop appears is assumed to be 3 times τ (Lhuissier and Villermaux, 2012). Hence it is now possible to calculate the average diameter of the drops generated by the fragmentation of the bubble (Eq. 27) (Lhuissier and Villermaux, 2012):

$$< d >= 2\sqrt{V \cdot \tau \cdot h} = 2 \cdot R^{\frac{3}{8}} \cdot h^{\frac{5}{8}} \tag{27}$$

It is also necessary taking into account that not all the bubbles will produce a consistent aerosol. From experimental data (Resch and Afeti, 1991; Spiel, 1998) two limit bubble radius R_{max} and R_{min} have been observed. Outside of those values, the respective bubbles will not be considered, since it will not contribute to the aerosol formation. Eqs. (28-29) report the correlations for the determination of such threshold limit value of bubble radius (Lhuissier and Villermaux, 2012).

$$\frac{R_{\min}}{a} \cong \left(2 \cdot 3^5 \cdot \frac{a}{\ell} \right)^{\frac{1}{3}} \tag{28}$$

$$\frac{R_{\max}}{a} \cong \left(\frac{2^8 \cdot 3^5}{7^2} \cdot \frac{\rho_{air} \cdot \ell}{\rho \cdot a} \right)^{\frac{1}{7}} \tag{29}$$

For the present study, R_{min} equal to 1mm and R_{max} is equal to 3.8*a*.

2.2.3. Aerosol characterization

Given all its geometric properties, it is possible to estimate the total volume of the liquid cap Ω in the bubble (Eq. 30):

$$\Omega \approx \frac{R^4 \cdot h}{a^2} \tag{30}$$

Since the mean diameter of the drops generated by the film rupture is known by Eq. (27) it is then possible to evaluate the number of drops N (Eq. 31), assuming that the whole film will scatter into drops (Lhuissier and Villermaux, 2012). This is not true in general.

$$N = 10^{-2} \frac{\Omega}{< d >^3} = 10^{-2} \cdot \left(\frac{R}{a} \right)^2 \cdot \left(\frac{R}{h} \right)^{\frac{7}{8}} \tag{31}$$

The drops released in the environment, will form both aerosol and fogs, and this is what mainly contributes to the source term.

The rearrangement of the drops diameter in the air can be assumed to follow a gamma distribution (Eqs. 32-33) (Lhuissier and Villermaux, 2012):

$$p\left(x = \frac{d}{< d >} \right) = \frac{n^n}{\Gamma(n)} x^{n-1} \cdot e^{-nx} \tag{32}$$

where

$$\Gamma(n) = \int_0^{\infty} t^{n-1} \cdot e^{-t} dt \tag{33}$$

Fig. 7 shows an example of gamma distribution (see Eq. 33) for 11 drops.

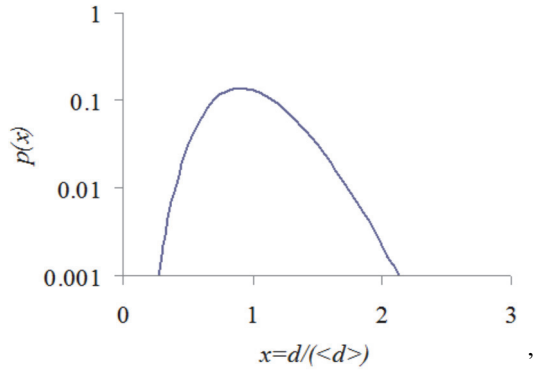

Fig. 7. Distribution p(x) for n=11

2.3. Source term estimation

Now it is possible to derive the final model for the source term of the galvanizing bath. We will now introduce a revised form of some quantity already presented. Particularly, we will refer to d_{ij} as the diameter of the *j*-th drop generated by the *i*-th bubble (Eq. 34).

$$d_{ij} = < d >_i \cdot x_j \tag{34}$$

N_{ij} is the number of drops with characteristic diameter *j* generated from each bubble *i*, using the normalized distribution p_n (Eq. 35):

$$N_{ij} = p_n(x)_j \cdot N_i \tag{35}$$

V_{ij} is the volume of a single drop j of the bubble *i*, V_i is the volume (Eqs. 36-37) of the entire bubble.

$$V_{ij} = N_{ij} \frac{\pi \cdot d_{ij}^{\ 3}}{6} \tag{36}$$

$$V_i = \sum_{j=R_{\min}}^{R_{\max}} V_{ij} \tag{37}$$

Some further assumption must be done in order to estimate the global emission:

- The distribution of the bubble size is estimated at first with a Poisson model, with X_i as the normalized probability for the bubble with radius *R* such that $R_{min}<R<R_{max}$, and $\aleph$ the probability that the bubble belongs to the interested range.
- The local extraction system has a capture efficiency equal to η.

It is now possible to define the total volume (Eq. 38) of the drops $\overline{V_i}$:

$$\overline{V_i} = \sum_{i=R_{\min}}^{R_{\max}} X_i \cdot V_i \tag{38}$$

Since we know the mixing air flowing for each tank *k*, it is possible to estimate the number of bubbles $\dot{n}$ generated over time (Eq. 39):

$$\dot{n} = \frac{Q_{mix_k} \cdot \aleph}{\overline{V_i}} \tag{39}$$

and the total number of drops extracted by each tank over time $\overline{V_k}$ (Eq. 40):

$$\overline{V_k} = \dot{n} \cdot \overline{V_i} \tag{40}$$

The source term of the *k*-th galvanizing tank for a component α is then calculable using Eq. (41):

$$G_{k\alpha} = V_k \cdot C_{k\alpha} \tag{41}$$

As it has been already said, the extraction system has a capture efficiency η, depending on several factors. Taking it into account we can estimate:

- Concentration (Eq. 42) in the extraction plenum of the pollutant α in the corresponding line μ.

$$C_{\mu\alpha} = \frac{\sum_{k\in\mu} G_{k\alpha}}{Q_\mu} \cdot \eta_k \tag{42}$$

- Source term for the entire environment from all the galvanizing tanks (Eq. 43):

$$\overline{V_k} = \dot{n} \cdot \overline{V_i} \tag{43}$$

2.4. Environmental concentration evaluation

Now that the new source term model has been defined, the next step consists in evaluating the concentration of the pollutant in the industrial area over time (C_α). Since the generation term $G_{dispα}$ is known, it is necessary to evaluate how it will affect the concentration in the air. Fig. 8 shows a schematization of the industrial area. For simplicity sake, we will consider a perfect mixing model that brings C_α as a function of the time only.

As done in section 2.1, we will determine the concentration of the pollutant, writing a material balance equation over the entire control volume (Eq. 44) (Goodfellow and Tähti, 2001).

$$acc = in - out + prod \tag{44}$$

where:

- *acc* is the accumulation term in the control volume (Eq. 45):

$$acc = \frac{d(m_\alpha)}{dt} = \frac{d(C_\alpha \cdot V)}{dt} = V \cdot \frac{d(C_\alpha)}{dt} \tag{45}$$

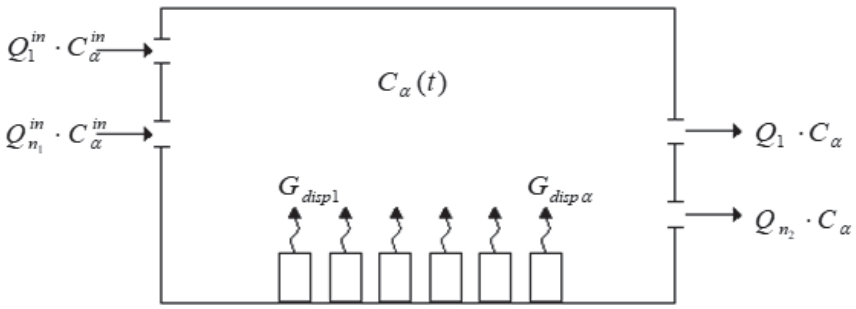

Fig. 8. Schematization of the anodizing baths with release of pollutants in the area

- *in* is the inlet flow rate of *α* inside the volume (Eq. 46). The contributes are given by the ventilation system, with possible different inlets *n* of air:

$$in = \dot{m}^{in} = \sum_n Q_{n_1}^{in} \cdot C_\alpha^{in} \tag{46}$$

- *out* is the outside mass flow rate of *α*, represented by the ventilation system (Eq. 47), with possible different outlets n_2 of air (note that, given the perfect mixing assumption, the concentrations are the same as the environmental ones):

$$out = \dot{m}^{out} = \sum_{n_2} Q_{n_2} \cdot C_\alpha \tag{47}$$

- *prod* is the production term $G_{disp\alpha}$ given by out model.

The mass balance (Eq. 48) becomes then (Goodfellow and Tähti, 2001):

$$V \cdot \frac{d(C_\alpha)}{dt} = \sum_n Q_{n_1}^{in} \cdot C_\alpha^{in} - \sum_{n_2} Q_{n_2} \cdot C_\alpha + G_{disp_\alpha} \tag{48}$$

This is another linear first order differential equation. The initial condition is (Eq. 49):

$$C_\alpha(t=0) = C_\alpha^0 = 0 \tag{49}$$

The analytical solution is (Eq. 50):

$$C_\alpha = C_\alpha^S - (C_\alpha^S - C_\alpha) \cdot \exp\left(\frac{-\sum_{n_2} Q_{n_2}}{V} t \right) \tag{50}$$

C_α^S is the stationary concentration (the derivative over time becomes zero), that is the concentration of the pollutant *α* (Eq. 51) after a certain amount of time:

$$C_\alpha^S = \frac{\sum_n Q_{n_1}^{in} \cdot C_\alpha^{in} + G_{disp_\alpha}}{\sum_{n_2} Q_{n_2}} \tag{51}$$

3. Results and discussion

A comparison between the results of the proposed model with some experimental data is repoted. The pollutants studied are: fluoridric acid, sulfuric acid, phosphoric acid, nitric acid and nichel, chromium (VI) ions. Two types of concentrations have been analyzed: extraction system and environmental concentrations. The first one is more reliable, the high turbulence in the exctraction system allows a uniform concentration in all the conduits, and the sample has very accurate values. The environmental concentrations, influenced by the fluid dynamics of the whole facility, are more scattered, thus less reliable, but we decided to take them into account aswell.

Table 1. Concentration [kg/m³] of substances for all the tanks

	Tank number									
	6	**9**	**13**	**15-16**	**17**	**22**	**24**	**31**	**33**	**35**
HF	2.1									1.05
H_2SO_4	6			99	99					
H_3PO_4	4.5									
HNO_3			90							0.75
CrO_3										4.5

Table 2. Characteristics of the tanks

	Tank number								
	6	**13**	**15-16**	**17**	**22**	**24**	**31**	**33**	**35**
Tank length [m]	0.85	0.75	2.3	1	0.85	0.85	0.85	0.85	0.85
Mixing flow [L/s]	17.8	17.6	54.0	23.5	19.9	19.9	22.8	22.8	22.8

Table 3. Physical properties of the bath solution

Physical properties of the solution	
σ[N/m]	0.073
ρ [kg/m^3]	1000
g [kg/m/s^2]	9.81
R [m]	0.0011:0.01036
ρ_{air} [kg/m^3]	1.225
a [m]	0.00273
Hydrostatic force [N/m]	0.00571
θ_C	1.096
Hydrostatic pressure [Pa]	101.640
Capillary pressure [Pa]	14.091
E	0.0001
l [m]	20

Table 4. Sampled concentration in the extraction systems for the two lines E01 and E02 through different years, with a total sampling time of 25 min (* average of three samples, < indicates that the real value is below the threshold)

	Sampling year					
	2013*		***2009***		***2006***	
Concentrations [mg/m^3]	E01	E02	E01	E02	E01	E02
HF		2.05E-01 ± 5.06E-02		7.30E-02± 5.06E-02		3.00E-02 ± 5.06E-02
H_2SO_4	3.93E-01± 9.70E-02		8.90E-02± 9.70E-02		<3.00E-02	
H_3PO_4	<4.00E-01		<1.70E-01		<3.00E-01	
HNO_3	4.37E-01± 2.00E-02		5.00E-01± 2.00E-02		1.00E-01± 2.00E-02	
Ni		9.57E-03 ± 2.36E-03		<3.60E-04		<1.00E-03
Cr(VI)		2.97E-02 ± 2.31E-03		7.40E-02± 2.31E-03		5.00E-03± 2.31E-03

Table 5. Predicted concentration in the extraction systems for the two lines E01 and E02 through different years

	Year					
	2013		2009		2006	
Air flow in E01 [m^3/s]	5.63		6.28		9.46	
Air flow in E02 [m^3/s]	5.17		5.35		3.81	
Concentration [mg/m^3]	E01	E02	E01	E02	E01	E02
HF	1.89E-03	6.67E-03	1.69E-03	6.73E-03	1.12E-03	9.44E-03
H_2SO_4	4.22E-01		3.79E-01		2.51E-01	
H_3PO_4	4.04E-03		3.63E-03		2.41E-03	
HNO_3	7.98E-02	9.40E-04	7.17E-02	9.08E-04	4.76E-02	1.27E-03
Ni		1.75E-03		1.68E-03		2.36E-03
Cr(VI)		2.93E-03		2.83E-03		3.98E-03

It is also importat to note that the processes have an intrinsic high variability, due to the importance of the human-based operations required. The proposed model was applied to the whole facility, including all the tanks used to perform the process. Table 1 represents the average concentration of poluttant for each tank, Table 2 shows the characteristics of the tanks. Table 3 lists all the solution parameters required for the model. The results from the model have been compared with a set of experimental data that have been collected for three years, 2006, 2009, 2013.

3.1. Extraction system concentrations

First, concentrations where studied in the extraction line of the facility. Table 4 shows all the concentration sampled from the two extraction systems lines (E01 and E02). The results of the simulation are reported in Table 5. For each simulation, the air flow was directly measured and applied.

We report in Fig. 9 a comparison among experimental and predicted values. At first, we can notice that the experimental results can be remarkably different among themselves. These differences are not simply justified by different values for the air flows, and reflects the volatility of the results, strictly related to how the process is performed by the operators. Anyways, we have good predictions for sulfuric acid (but it is overestimated) and nickel (Figs. 9b and e). Also 2006 data tend to show a good agreement with almost all the predictions.

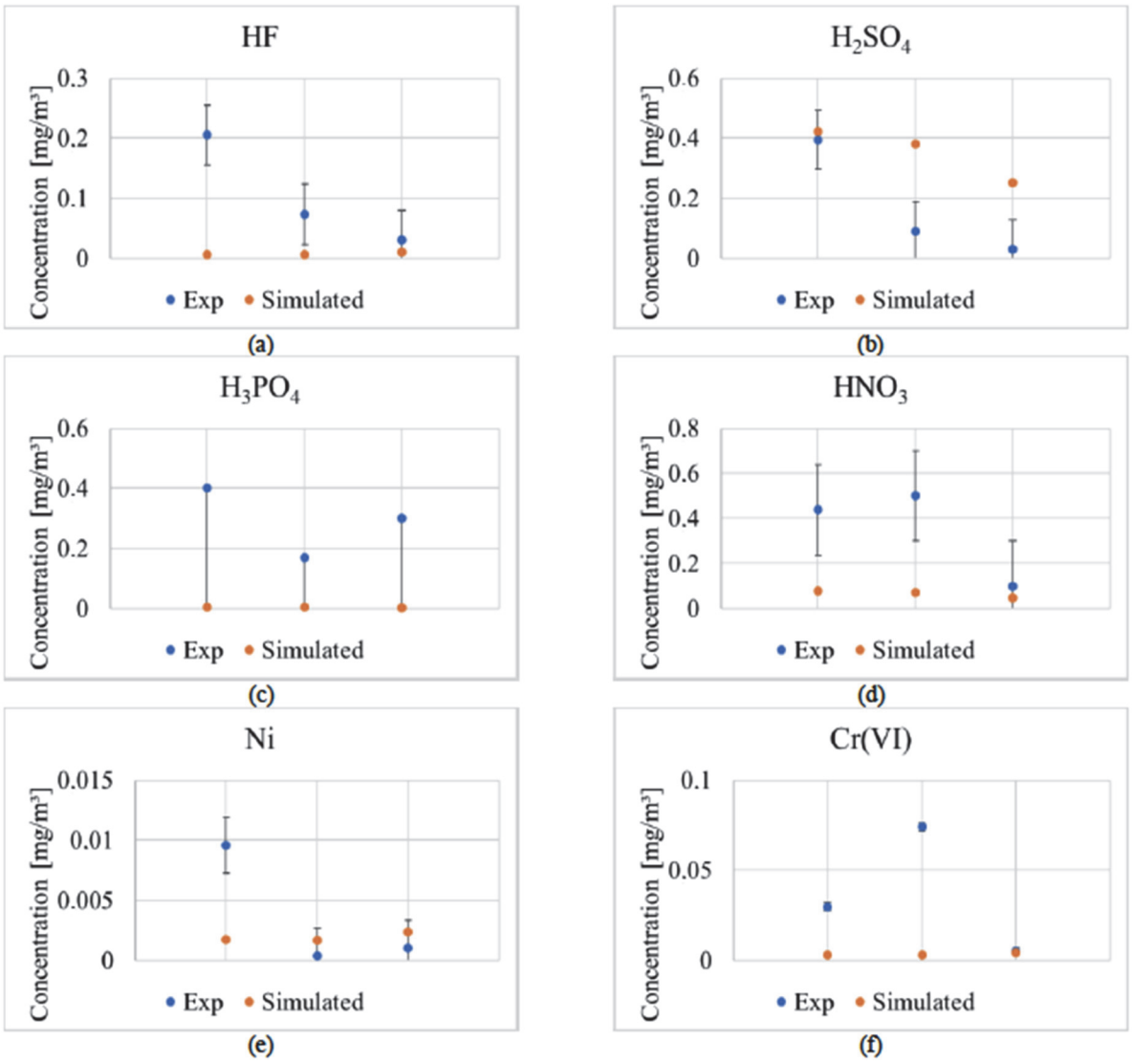

Fig. 9. Comparison among experimental and simulated data for the pollutants concentrations at extraction points (from left ot right: 2013, 2009, 2006)

Table 6. Sampled concentrations in the environment for personal samplers (P01, P02), environmental samplers (A01) in different years (sampling time is between 120 and 150 min, < indicates that the real value is below the threshold)

Year	***2013***			***2009***		
Concentrations [mg/m³]	A01	P01	P02	A01	P01	P02
H_2SO_4	2.10E-01± 4.20E-02			<6.80E-02		
HNO_3	1.20E-01± 2.40E-02			1.60E-01± 3.20E-02		
Ni	1.60E-04± 3.20E-05	<1.50E-03	<1.50E-03	3.00E-04± 6.00E-05	<1.50E-03	<1.50E-03
Cr(VI)		<1.60E-03	<1.60E-03		<3.00E-02	<3.00E-02
Year	***2006***					
Concentrations [mg/m³]	A01	P01	P02			
H_2SO_4	6.00E-02± 1.20E-02					
HNO_3	1.10E-01± 2.20E-02					
Ni	<2.00E-03	<2.00E-03	<3.00E-03			
Cr(VI)		<1.00E-02	<3.00E-03			

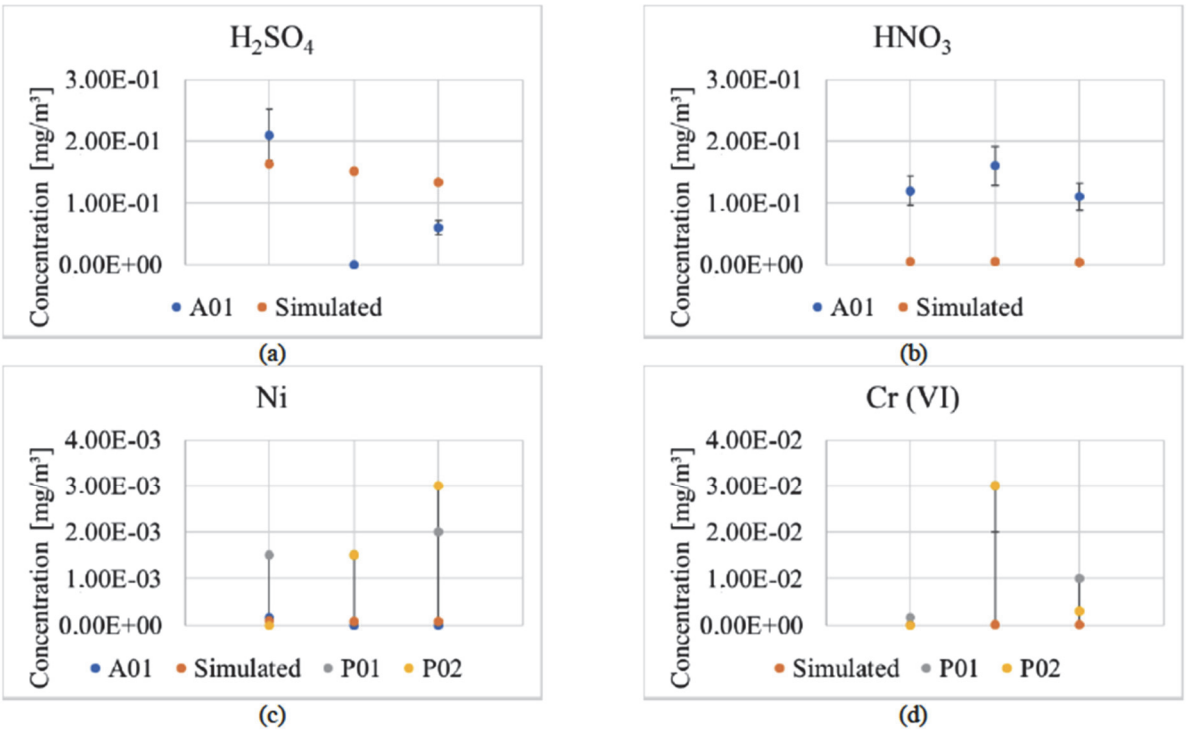

Fig. 10. Comparison among experimental and simulated data for environmental concentrations (from left ot right: 2013, 2009, 2006) (A01: environmental sampler, P01,P02: personal sampler)

In addition, we notice that HF concentration is always underestimated by the model. For phosphoric acid, real values are below the threshold reported, hence significant information cannot be deducted. In the end, we have consistent discrepancies for nitric acid. In this case, there is a reasonable explanation: nitric acid is subject of complex decomposition reactions, which are not considered in the model.

3.2. Environmental concentrations

The concentration in the indoor environment, highly depends on the fluid dynamics of the system. The model, for simplicity issues, uses perfect mixing and stationary state as assumptions, but it is far distant from the real case: in a real building we have several dead points, internal recirculation and radiant convective flows that interact with the dispersion phenomenon. For this reason, both personal samplers (P02, P02) and environmental samplers (A01) have been applied to obtain experimental concentrations of sulfuric and nitric acid, nickel and chromium. A wider set of data is supposed to give a better interpretation of the results of our model. In Table 6 we have the experimental values and in Table 7 the result of the model. The physical properties are the same as above. The additional datum required now is the general ventilation air flow, which was directly measured in the facility (Table 7).

We can see that environmental and personal samplers bring often to different results, highligthning the volatility of the measurements. Personal samplers give similar values. Fig. 10 compares the different results including band errors, where available.

Again, we confirm good estimation for sulfuric acid concentrations, with a slight overestimation overall (Fig. 10a). For nickel, we have a decent comparison with environmental samplers (Fig. 10c). About personal samplers, not much can be said, since all the experimental values are below the instrument threshold. Same goes for chromium values. For nitric acid, we still have underestimation of the experimental values, possibly due to the decomposition reactions not included in this study.

Table 7. Simulated concentrations in the environment in different years

Year	*2013*	*2009*	*2006*
Ventilation air flow[m^3/s]	10.81	11.63	13.28
Concentrations [mg/m^3]			
H_2SO_4	1.63E-01	1.52E-01	1.33E-01
HNO_3	4.68E-03	4.35E-03	3.81E-03
Ni	9.27E-05	8.62E-05	7.55E-05
Cr(VI)	1.56E-04	1.45E-04	1.27E-04

4. Conclusions

A model to estimate the source term of pollutants in a galvanic process has been analyzed. In particular, the model considers as the main phenomenon that regulates the dispersion of pollutants in the environment, the rupture of the bubbles in the galvanizing baths, that emerging up to the liquid surface are subsequently broken. A facility where both anodizing and chromate conversion coating of aluminium processes are carried out has been considered as case study. The results of the model have showed a good agreement with the data sampled

directly in the facility, for what concern sulfuric and nitric acid, nickel and chromium concentrations. Nitric acid did not give interesting results, but it is due to its peculiar decomposition reactions, that were not taken into account in the current model.

This work opens the way to future improvements. It would be interesting to develop more specific models (i.e. nitric acid), taking in account the fluid dynamic of the bubbles that rise from the sparger to the liquid surface, in order to predict with increasing precision the real environmental concentration of harmful agents in the galvanic industry.

List of letters and symbols

a	Capillary length, m
A	Grouping (see Eq. 18)
α	Generic pollutant Aluminium oxide form
B	Aluminium oxide form Grouping (see Eq. 19)
C	Molar concentration, kmol/m^3
C_α	Molar concentration of α, kmol/m^3
C_α^0	Molar concentration of α at starting time (see Eq. 16), kmol/m^3
C_α^S	Molar concentration of α at steady state, kmol/m^3
$C_{\mu\alpha}$	Molar concentration of α in the extraction plenum, in the μ-th line of the extraction system, kmol/m^3
C_α^{in}	Molar concentration of α in the inlet air, kmol/m^3
D	Drop diameter, m
d_b	Diameter of the bubbles generated by the sparger, m
d_0	Sparger pore diameter, m
$<d>$	Average drop diameter, m
Δ	Pinch thickness, m
E	Puncture efficiency, -
F	Force, N
F_b	Buoyant force, N
F_{sur}	Surface tension force on the base of a bubble, N
$F(\theta)$	Geometric factor of the bubble, -
G	Gravitational acceleration, m/s^2
$G_{k\alpha}$	Source term for α in the k-th bath, mol/s
$G_{disp\alpha}$	Source term for α, mol/s
Γ	Aluminium oxide form Centripetal acceleration (see Eq. 30), m/s^2
$\Gamma(n)$	Gamma function (see Eq. 41)
H	Average bubble film thickness, m
h_b	Limit bubble film thickness, m
H	Capture efficiency, -
η_k	Capture efficiency of the k-th tank, -
K	Generic galvanizing tank
k_p	Mass transport coefficient, m/s
l	Pinching length, m
ℓ	Characteristic length, m
λ	Instability wave length, m
$\dot{m}^{in}$	Molar incoming flow rate, mol/s
$\dot{m}^{out}$	Molar outcoming flow rate, mol/s
μ_l	Liquid viscosity, Pa·s
n	Shape and rate parameter of the gamma distribution (see Eq. 40)
$\dot{n}$	Bubbles generation rate, 1/s
n_1	Number of inlets in the general ventilation system, -
n_2	Number of outlets in the general ventilation system, -
N	Number of drops generated by a bubble rupture, m
$\aleph$	Probability that a bubble has a radius R so that $R_{min}<R<R_{max}$
Ω	Volume of liquid contained in a bubble film, m^3
P	Pressure, Pa
P^0_α	Vapor pressure, Pa
PM_α	Molecular weight of α, kg/kmol
Q_{airmix}	Volumetric flow rate of the mixing air in the tank, m^3/s
Q_{extr}	Volumetric flow rate of the extraction system in the tank, m^3/s
Q_{mixk}	Volumetric flow rate of the mixing air in the k-th tank, m^3/s
Q_μ	Volumetric flow rate in the plenum of the μ-th line of the extraction system, m^3/s
Q_{extr}	Volumetric flow rate of the extraction system in the tank, m^3/s
Q_{mixk}	Volumetric flow rate of the mixing air in the k-th tank, m^3/s
Q_{n1}^{in}	Volumetric flow rate of the air in the general ventilation in the n_1-th inlet
Q_{n2}	Volumetric flow rate of the air in the general ventilation in the n_2-th outlet
$\overline{R}$	Ideal gas constant = 8.314, kJ/(kmol·K)
R	Bubble radius of curvature, m
R_{min}	Minimum radius (see Eq. 36), m
R_{max}	Maximum radius (see Eq. 37), m
ρ	Density of a liquid/solution/water, Kg/m^3
ρ_{air}	Density of air, Kg/m^3
S_{evap}	Evaporating liquid surface, m^2
σ	Surface tension, N/m
t	Time, s
T	Temperature, K
τ	Capillary time, s
θ_C	Characteristic angle of a bubble, rad
V	Volume (liquid, bubbles, drops, facility etc..), m^3
v	Taylor-Culick velocity, m/s
x	Gamma distribution variable, (see Eq. 40)
X	Normalized Poisson distribution variable
y	Poisson variable for bubble diameter distribution, (see Eq. 21)

References

Bergstra A.D., Brunekreef B. Burdorf A., (2018), The mediating role of risk perception in the association between industry-related air pollution and health, *PLoS ONE*, **13**, e0196783.

Culick F.E.C., (1960), Comments on a ruptured soap film, *Journal of Applied Physics*, **31**, 1128-1129.

Cioca L.I., Moraru R.I., Babuţ G.B., (2010), *Occupational Risk Assessment: A Framework for Understanding and Practical Guiding the Process in Romania*, Proc. of the International Conference on Risk Management, Assessment and Mitigation, RIMA '10, Bucharest, Romania, 56-61.

Cioca L.I., Ivascu L., (2016), Investigating occupational diseases in the metallurgical industry, *Metalurgija*, **55**, 852-854.

Cioca L.I., Ivascu L., Rada E.C., Torretta V., Ionescu G., (2015), Sustainable development and technological

impact on CO_2 reducing conditions in Romania, *Sustainability*, **7**, 1637-1650.

Călămar A., Găman G.A., Toth L., Pupăzan D., Simion S., (2016), *Assessment of Workers' Occupational Exposure in the Context of Industrial Toxicology*, Proc. IOP Conference Series: Earth and Environmental Science, **44**, 032004.

Călămar A.-N., Găman G.A., Pupăzan D., Toth L., Kovacs I., (2017), Analysis of environmental components by monitoring gas concentrations in the environment, *Environmental Engineering and Management Journal*, **16**, 1249-1256.

Călămar A.-N., Toth L., Găman G.-A., Kovacs M., (2018), Analysis of olfactive discomfort, generated by industrial activities neighboring residential areas, affecting the quality of life and health of population, *International Multidisciplinary Scientific GeoConference Surveying Geology and Mining Ecology Management*, SGEM, **18**, 35-42.

Cocarta D.M., Rada E.C., Ragazzi M., Badea A., Apostol T., (2009), A contribution for a correct vision of health impact from municipal solid waste treatments, *Environmental Technology*, **30**, 963-968.

Diggle J.W., Downie T.C., Coulding C.W., (1969), Anodic oxide films on aluminum, *Chemical Reviews*, **69**, 365-405.

DEHP, (1998), Galvanizing processes, Department of Environmental and Heritage Protection, Government of Queensland, Sydney, Australia.

DSEWPC, (2012), *Emission Estimation Technique Manual for Galvanizing*, Department of Sustainability, Environment, Water, Population and Communities, Australian Government.

Goodfellow H., Tähti E., (2001), *Industrial Ventilation Design Guidebook*, Academic Press, San Diego, USA.

Jang Y.-C., Shin Y., Kim H., Lee J.-H., (2017), Human health risk assessment of arsenic in air, soil and water in an industrial complex in Korea, *Environmental Engineering and Management Journal*, **16**, 293-301.

Junaid M., Hashmi M.Z., Malik R.N., (2016), Evaluating levels and health risk of heavy metals in exposed workers from surgical instrument manufacturing industries of Sialkot, Pakistan, *Environmental Science and Pollution Research*, **23**, 18010-18026.

Fontcha D.S., Spooner K., Salemi J.L., Naik E., Aliyu M.H., Mogos M.F., Zoorob R., Salihu H.M., (2015), Industry-Related Injuries in the United States from 1998 to 2011: Characteristics, trends, and associated health care costs, *Journal of Occupational and Environmental Medicine*, **57**, 814-826.

Kumar R., Kuloor N.R., (1970), *The Formation of Bubbles and Drops*, In*: Advances in Chemical Engineering*, vol. 8, Academic Press, New York, USA.

Lhuissier H., Villermaux E., (2012), Bursting bubble aerosol, *Journal of Fluid Mechanics*, **696**, 5-44.

Matarazzo A., Clasadonte M.T., Ingrao C., (2018), The (Dominance based) rough set approach applied to air pollution in a high risk rate industrial area, *Environmental Engineering and Management Journal*, **17**, 591-599.

Moraru R.I., Băbuţ G.B., Cioca L.I., (2014), Rationale and criteria development for risk assessment tool selection in work environments, *Environmental Engineering and Management Journal,* **13**, 1371-1376.

Nierstrasz V.A., Frens G., (1998), Marginal regeneration in thin vertical liquid films, *Journal of Colloid and Interface Science*, **207**, 209-217.

Oprea M., Dunea D., Liu H.-Y., (2017), Development of a knowledge based system for analyzing particulate matter air pollution effects on human health, *Environmental Engineering and Management Journal*, **16**, 669-676.

Perry R.H., Green Don W., (2007), *Perry's Chemical Engineers' Handbook*, 8th edition, Mc Graw Hill, New York, USA.

Rada E.C., Ragazzi M., Schiavon M., (2014), Assessment of the local role of a steel making plant by POPs deposition measurements, *Chemosphere*, **110**, 53-61.

Resch F., Afeti G., (1991), Film drop distribution from bubbles bursting in seawater, *Journal of Geophysical Research*, **96**, 10681-10688.

Schiavon M., Ragazzi M., Rada E.C., Torretta V., (2016), Air pollution control through biotrickling filters: a review considering operational aspects and expected performance, *Critical Reviews in Biotechnology*, **36**, 1143-1155.

Schiavon M., Ragazzi M., Rada E.C., Magaril E., Torretta V., (2018), Towards the sustainable management of air quality and human exposure: Exemplary case studies, *WIT Transaction on Ecology and Environment*, **230**, 489-500.

Stefan S., Barladeanu R., Andrei S., Zagar L., (2015), Study of air pollution in Bucharest, Romania during 2005-2007, *Environmental Engineering and Management Journal*, **14**, 809-817.

Torretta V., Rada E.C., Capodaglio A.G., (2015), An example of the use of bio-indicators for air quality assessment in areas with high industrial presence, *Environmental Engineering and Management Journal*, **14**, 2679-2687.

Shareefdeen Z., Singh A., (2004) *Biotechnology for Odor and Air Pollution Control*, Heidelberg, Springer, New York, USA.

Simion S., Kovacs M., Toth L., Ilie C., Gireadă A., (2017), Workers exposure to noise in surface extractive industry, *Environmental Engineering and Management Journal*, **16**, 1367-1372.

Spiel D.E., (1998), On the birth of film drops from bubbles bursting on seawater surfaces, *Journal of Geophysical Research: Oceans*, **103**, 24907-24918.

TCEQ, (2018), *Calculation guidance package, Hot dip galvanizing*, Texas Commission on Environmental Quality, Air Permits Division, Austin, USA.

USEPA, (1995), *Compilation of Air Pollutant Emission Factors, Volume 1: Stationary Point and Area Sources, Fifth Edition, AP-42, Section 12.14 Secondary Zinc Processing*, United States Environmental Protection Agency, Office of Air Quality Planning and Standards.

Volk P., (2013), *Replacement of Hexavalent Chromium*, TSB Project Meeting in Lboro, SurTec International. Loughborough, UK. On line at: https://www.surtec.com/ecomaXL/files/surtec_102429862113829504202013-08-20_TSB_HiTEA_group_meeting_Loughborough.pdf&download=1.